Am J Transl Res 2019;11(5):2908-2924
www.ajtr.org /ISSN:1943-8141/AJTR0090008

Original Article

In vitro transdifferentiation of adipose tissue-derived stem cells into salivary gland acinar-like cells

Tai-Qiang Dai[1*], Lin-Lin Zhang[2*], Ying An[2], Fang-Fang Xu[1], Ran An[3], Hai-Yan Xu[3], Yan-Pu Liu[1], Bin Liu[3]

[1]*State Key Laboratory of Military Stomatology & National Clinical Research Center for Oral Diseases & Shaanxi Clinical Research Center for Oral Diseases, Department of Oral and Maxillofacial Surgery, School of Stomatology, The Fourth Military Medical University, Xi'an 710032, PR China;* [2]*State Key Laboratory of Military Stomatology & National Clinical Research Center for Oral Diseases & Shaanxi Engineering Research Center for Dental Materials and Advanced Manufacture, Department of Periodontology, School of Stomatology, The Fourth Military Medical University, Xi'an 710032, PR China;* [3]*State Key Laboratory of Military Stomatology & National Clinical Research Center for Oral Diseases, Laboratory Animal Center, School of Stomatology, The Fourth Military Medical University, Xi'an 710032, PR China.* [*]*Equal contributors.*

Received December 17, 2018; Accepted March 26, 2019; Epub May 15, 2019; Published May 30, 2019

Abstract: Current clinical approaches to treat irradiation-induced salivary gland hypofunction are ineffective. We previously reported that adipose-derived stem cell (ADSC)-based therapy ameliorates damaged salivary gland function in mice and that the effects were enhanced when the therapy was co-administrated with platelet-rich fibrin (PRF). We examined the feasibility of ADSC transdifferentiation into salivary gland acinar-like cells (SGALCs) and analyzed the potential of PRF to promote the transdifferentiation process in vitro. Salivary gland cells (SGCs) and ADSCs were indirectly co-cultured using Transwell inserts, and increasing concentrations of PRF-conditioned medium were applied to the co-culture system. The expression of α-amylase and AQP-5 were used to evaluate ADSC transdifferentiation. Notably, on day 7, 14, and 21, expression of both α-amylase and AQP-5 were detected in the co-cultured ADSCs. Additionally, PRF increased α-amylase and AQP-5 levels in ADSCs that were co-cultured for 7 days. These data demonstrate that ADSCs have the potential to transdifferentiate into SGALCs and that PRF can promote the transdifferentiation process. Therefore, these data reveal a possible mechanism to treat irradiation-induced salivary gland hypofunction and have translational medicine implications.

Keywords: Salivary gland cells, adipose-derived stem cells, platelet-rich fibrin, co-culture, transdifferentiation

Introduction

Head and neck cancer is one of the most prevalent cancers worldwide and due to its location, many patients receive radiotherapy treatment. However, radiotherapy induces irreversible damage to the salivary glands (SGs). The SGs are one of the most important types of exocrine glands in the human body because they secrete saliva, which has vital roles in chewing, swallowing, speaking, and digestion [1]. Radiation-induced damage to the SGs decreases saliva secretion. Consequently, patients develop xerostomia and dental caries, and experience difficulties chewing and swallowing, which collectively decreases their quality of life [2]. Current clinical management strategies for SG hypofunction are limited to sialagogue use [3] (for example, pilocarpine, which can stimulate the function of residual SGs), oral lubricants, saliva substitutes [4], and physical treatments [5, 6]. However, these strategies do not significantly improve SG function and they are often accompanied by undesirable side effects [7].

Currently, the role of stem cells in tissue repair and function restoration is an active area of study. In particular, bone marrow mesenchymal stem cells (BMMSCs) and adipose tissue-derived stem cells (ADSCs) have attracted considerable attention. However, ADSCs are more suitable for practical use because they are easily acquired in large quantities [8]. In addition, ADSCs exhibit better immunomodulatory properties [9]. Several studies have demonstrated that ADSCs can promote tissue repair and re-

generation in a variety of diverse contexts that include [10] bone [11], cartilage [12], nerve [13], liver [14], and heart [15] tissues. Furthermore, ADSCs improve SG malfunction. Direct administration of ADSCs into the submandibular glands of C57BL/6 mice improved saliva flow rate and blood vessel proliferation after SG irradiation injury [16]. Similar functional improvements in irradiated SGs were observed after intraglandular transplantation of ADSCs in Sprague-Dawley rats [17]. Finally, systemic transplantation of ADSCs using tail-vein injections protected against irradiation-induced cell loss and improved saliva flow rate and salivary gland microstructure [18]. Despite achieving functional improvements in damaged SGs, the current state of ADSC-based therapy is insufficient for clinical applications.

Platelet-rich fibrin (PRF) is a second generation platelet concentrate that is obtained from the middle layer of blood samples after centrifugation at 3,000 rpm [19]. The three-dimensional structure of PRF is extremely complex. Fibrin and various growth factors, including transforming growth factor-β1 (TGF-β1), platelet-derived growth factors (PDGFs), insulin-like growth factor-1 (IGF-1), and vascular endothelial growth factor (VEGF), are trapped within the intricate PRF structure [20]. Due to its three-dimensional structure and the presence of numerous growth factors, PRF contributes to tissue healing and regeneration processes including wound healing [21], angiogenesis [22], and the regeneration of bone [23], cartilage [24], and periodontal tissues [25]. Furthermore, PRF can stimulate the proliferation and differentiation of several cell types including osteoblasts [26], oral bone mesenchymal stem cells [27], and dental pulp cells [28].

Previously, we observed that immediate intravenous administration of ADSCs after local SG irradiation improved gland morphology and function in mice [29]. In addition, when combined with PRF, the ADSCs were more effective at ameliorating irradiation-induced SG damage (in press). However, the mechanisms that contribute to rescued SG function after ADSC treatment remain unknown. Because ADSCs can transdifferentiate into several different cell types, including cardiomyocyte-like cells [30], Schwann-like cells [31], and urothelium-like cells [32], we hypothesized that ADSCs may have the potential to transdifferentiate into salivary gland acinar-like cells (SGALCs). Furthermore, PRF may promote the transdifferentiation of ADSCs in SGALCs.

The aim of the current study was to investigate the underlying mechanisms of ADSC-based therapy that ameliorates damaged salivary gland function. We co-cultured SGCs and ADSCs with Transwell inserts and added PRF-conditioned medium to the co-culture system to determine the transdifferentiation potential of ADSCs in the presence of PRF. Our data indicate that ADSCs transdifferentiate into SGALCs and that the process is enhanced in the presence of PRF.

Material and methods

Ethics statement

Four-week-old C3H mice were used as the cell sources for the in vitro experiments. New Zealand rabbits were used to acquire PRF. All animals were treated according to protocols approved by the Animal Care and Use Committee at the Fourth Military Medical University, Xi'an, China.

Isolation and culture of mouse ADSCs

Adipose tissue was obtained from the inguinal fat pads of C3H mouse. The ADSCs were isolated and cultured as previously described [33]. Briefly, the fat pads were washed twice with phosphate buffered saline (PBS) and the additional fascia and blood vessels were removed. The remaining tissue was then minced, followed by digestion with collagenase (0.1%, type I; Sigma-Aldrich, St. Louis, MO, USA) for 40 min with vigorous shaking at 37°C in a conical flask. The resulting cell suspensions were filtered through a 75-μm mesh and centrifuged at 1,000 rpm for 5 min. The cell pellets were washed twice, followed by resuspension in Dulbecco's Modified Eagle Medium (DMEM, Gibco, Carlsbad, CA, USA) supplemented with 10% fetal bovine serum (FBS, Biowest, Nuaillé, France) and 1% penicillin-streptomycin (penicillin, 100 U/ml; streptomycin, 100 μg/ml; Hyclone, Logan, Utah, USA). Then, the cell suspensions were plated on 100-mm cell culture dishes (Corning, Lowell, MA, USA) and incubated at 37°C in a 5% CO_2 and 100% humidified atmosphere. The culture medium was changed every 2 or 3 days. The cells were sub-cultured at a

ratio of 1:2 at 80% confluency. Passage 3 ADSCs were used for all cell experiments.

Identification of ADSCs

The ADSCs were differentiated into adipogenic, osteogenic, and chondrogenic lineages. Passage 3 ADSCs were cultured to confluency in DMEM with 10% FBS in 6-well plates, followed by induction with the appropriate media. For adipogenic differentiation, confluent ADSCs were cultured in DMEM containing 10% FBS, 0.5 mM 3-isobutyl-1-methylxanthine, 1 μM dexamethasone, 10 μM insulin, 0.1 mM indomethacin (all from Sigma-Aldrich, USA), and 1% penicillin-streptomycin. After 3 weeks, the cells were stained with Oil Red-O (Sigma-Aldrich, USA) to identify adipogenic differentiation. For osteogenic differentiation, the ADSCs were cultured in DMEM supplemented with 10% FBS, 0.1 μM dexamethasone, 10 mM β-glycerophosphate, 50 μM L-ascorbate-2-phosphate (all from Sigma-Aldrich, USA), and 1% penicillin-streptomycin for 3 weeks. Then, the cells were stained with Alizarin red (Kermel, Tianjin, China) to identify osteogenic differentiation. Chondrogenic induction was performed using the pellet method. Briefly, 2×10^5 ADSCs were pelleted in the bottom of a 15-mL tube. After culturing in DMEM containing 10% FBS for 24 h, the ADSC pellet was induced for 21 days in DMEM containing 10% FBS, 1% ITS (insulin-transferrin-selenium, Gibco), 37.5 μg/mL L-ascorbate-2-phosphate (Sigma), 1 mM sodium pyruvate (Sigma), 10^{-7} dexamethasone (Sigma), and 10 ng/mL TGF-β1 (PeproTech, Rocky Hill, NJ, USA). The cell pellet was fixed with 4% paraformaldehyde and embedded in paraffin for cell staining. Five micrometer-thick sections of the ADSC pellet were stained with Alcian blue to identify chondrogenic differentiation.

For flow cytometry analysis, passage 3 ADSCs were harvested and resuspended at a concentration of 10^6 cells/mL. Samples containing 5×10^5 cells/100 μL were incubated at 4°C for 45 min with the following fluorescein isothiocyanate (FITC) and phycoerythrin (PE)-conjugated anti-mouse antibodies: CD29-PE, CD31-FITC, CD34-PerCP-Cy5.5, CD44-PE, CD45-PE, CD90-PE, and CD105-FITC (all from Biolegend, San Diego, CA, USA). Then, the cells were washed, resuspended, and analyzed using a flow cytometer (Beckman Coulter, Fullerton, CA, USA).

Isolation and culture of mouse SGCs

C3H mice were anesthetized using an intraperitoneal injection of sodium pentobarbital. Under sterile conditions, the submandibular glands were removed through a middle incision in the neck. Then, the SGCs were isolated and cultured as described previously, with slight modifications [34]. Briefly, the SGs were rinsed twice with PBS, and the fat and connective tissues were removed from the glands. The isolated glands were cut into small cubic pieces that had an approximate volume of 1 mm^3, resuspended in collagenase (0.1%, type II; Sigma-Aldrich, USA), and digested on a table shaker for 40 min at 37°C. After dispersion, the cells were filtered through a 75-μm mesh, washed twice, centrifuged at 1,000 rpm for 5 min, and finally resuspended in culture medium. The culture medium consisted of DMEM (Gibco) supplemented with 10% FBS (Biowest, France), insulin (5.0 μg/mL, Sigma-Aldrich), transferrin (5.0 μg/mL, Sigma-Aldrich), hydrocortisone (0.4 μg/mL, Sigma-Aldrich), epidermal growth factor (10 ng/mL, PeproTech), and 1% penicillin-streptomycin. The cell suspensions were plated in 100-mm culture dishes (Corning, USA) and cultured at 37°C in a humidified incubator with a 5% CO_2 atmosphere. The culture medium was changed every 2 or 3 days. At confluence, the cells were detached by trypsinization and were used for SGCs identification or co-culture.

Preparation of lyophilized PRF and PRF-conditioned medium

Fresh PRF clots were obtained according to the protocol by Choukroun et al. [35]. Briefly, 20 mL blood samples were collected from New Zealand rabbits and centrifuged immediately at 3,000 rpm for 10 min in two 10-mL glass tubes without anticoagulants. After centrifugation, there were three layers in the tubes: red blood cells comprised the bottom layer, PRF clots were in the middle layer, and acellular plasma was on the surface. The fresh PRF clots were separated from the other two layers and transferred into sterile 100-mm culture dishes, followed by freeze-drying for 24 h to obtain lyophilized PRF. The lyophilized PRF was ground and filtered through a 150-μm mesh to create small particles. To prepare conditioned medium, 25 mg of the lyophilized PRF particles were soaked

in 1 mL of fresh DMEM medium without FBS or the penicillin-streptomycin antibiotic.

Release of growth factors into lyophilized PRF particles

VEGF and PDGF-BB were selected to evaluate growth factor release. Samples were collected from the PRF-conditioned medium on day 0, 1, 2, 3, 5, 7, 9, 11, 14, 17, and 21. The samples were then centrifuged and the supernatants were transferred into new Eppendorf tubes, followed by rapid freezing at -80°C. There were three tubes for duplicate samples at every time point. Finally, VEGF and PDGF-BB levels in the samples were measured using commercial enzyme-linked immunosorbent assay (ELISA) kits (Sen Xiong Biotechnology, Shanghai, China). VEGF and PDGF-BB levels were determined according to the manufacturer's protocol. Briefly, the standards and samples of three duplicates were added to the assay plate wells and diluted. The assay plates were incubated at 37°C for 2 h, washed, and then incubated with enzyme-conjugated antibodies to VEGF and PDGF-BB for 1 h. Next, the wells were filled with substrate solution and incubated at 37°C for 20 min in dark. The stop solution was added to each well and absorption values at 450 nm were measured using an ELISA reader (Thermo Fisher Scientific, Waltham, MA, USA). The absorbance values were converted into concentrations of VEGF and PDGF-BB to create growth factor release curves.

Effects of lyophilized PRF on ADSCs proliferation and osteogenic differentiation

PRF-conditioned medium supernatants were collected on day 3 to evaluate the effect of PRF on ADSCs proliferation and osteogenic differentiation. To quantify proliferation, ADSCs was seeded in 96-well plates at a density of 2×10^3 cells/well and tested using the 3-(4,5-dimethylthiazol-2-yl)-2,5-diphenyltetrazolium bromide (MTT) assay. There were 10 groups for the MTT assay: One control group with normal culture medium (DMEM with 10% FBS) and nine groups with different concentrations of PRF-conditioned medium (0.5%, 1%, 3%, 5%, 7%, 10%, 20%, 50%, and 80%; the percentages indicate the volume ratio of the conditioned medium to stock DMEM). In each group, 10 wells were prepared for duplicate testing and one well was designated for the control. After culturing the cells with only DMEM containing 10% FBS for the first day, the cells were then cultured with different concentrations of conditioned medium, as specified above, from day 2-9. The conditioned culture medium was refreshed every 2 days. The MTT assay was performed daily for 9 days to monitor cell proliferation, and the spectrophotometric absorbance was read at 490 nm using an ELISA reader. Finally, growth curves were generated from the absorbance values, and the absorbance values on day 1, 2, and 8 were used for statistical comparisons.

For osteogenic differentiation, the ADSCs were seeded in 6-well plates and cultured to confluence in DMEM supplemented with 10% FBS. Then, the cells were refreshed with osteogenic induction medium containing different concentrations of PRF-conditioned medium (0%, 0.5%, 1%, 3%, 5%, 7%, and 10%). The mRNA levels of osteogenesis-related genes, including alkaline phosphatase (ALP), collagen I (COL I), runt-related transcription factor 2 (RUNX2), and osteocalcin (OCN) were assessed using quantitative reverse transcription-polymerase chain reaction (qRT-PCR) after 7 days of induction. The cells were stained with Alizarin red after 21 days of culture in osteogenic induction medium.

Co-culture of SGCs and ADSCs

Passage 3 ADSCs and passage 1 SGCs were co-cultured in a double-chamber system built using Transwell inserts that had a pore size of 0.4 μm (Millipore, Billerica, MA, USA). SGCs were cultured in the upper chamber and ADSCs were cultured in the lower chamber at a cell ratio of 4:1, respectively. The cells were cultured without direct interaction, and the system only permitted the transmission of soluble factors between the two compartments. The control group was cultured ADSCs in the lower chamber without SGCs in the upper chamber. The culture medium was DMEM supplemented with 10% FBS and 1% penicillin-streptomycin. ADSCs in the lower chamber were analyzed on co-culture day 7, 14, and 21. Cell density varied between different co-culture days and culture plates (**Table 1**).

To analyze the effect of PRF on the transdifferentiation of ADSCs into SGALCs, a 7-day co-culture system was used. DMEM supplemented with 10% FBS, containing different concentra-

Table 1. Number of SGCs and ADSCs in the co-culture system on different days

	Number of SGCs		Number of ADSCs	
	24-well plate	6-well plate	24-well plate	6-well plate
Day 7	2×10^4	8×10^4	5×10^3	2×10^4
Day 14	1.6×10^4	6×10^4	4×10^3	1.5×10^4
Day 21	1.2×10^4	4×10^4	3×10^3	1×10^4

tions of PRF-conditioned medium (0%, 0.5%, 1%, 3%, and 5%) was supplied to the co-cultured cells. To confirm that PRF did not affect the transdifferentiation of ADSCs in the absence of SGCs, a control group without SGCs in the upper chamber, but containing 1% PRF-conditioned medium was used. ADSCs were collected for analysis after 7 days of co-culture. The SGC groups were used as positive controls for quantification of α-amylase and AQP-5 levels.

Immunofluorescence staining

SGCs and ADSCs that were separately cultured on slides, ADSCs that were co-cultured for 7, 14, and 21 days, and ADSCs that were co-cultured for 7 days in PRF-conditioned medium were analyzed with immunofluorescence staining. The cells were washed twice with PBS and fixed with 4% paraformaldehyde for 20 min at room temperature. After washing with PBS, the cells were permeabilized with 0.1% Triton X-100 for 10 min to facilitate intracellular staining. The permeabilization process was omitted for AQP-5 staining. Then, the samples were washed, and non-specific binding was blocked with 10% goat serum (Biosynthesis Biotechnology, China). The slides containing the SGCs and ADSCs were then incubated overnight at 4°C with the following primary antibodies: polyclonal rabbit anti-α-amylase antibody, polyclonal rabbit anti-CK8 antibody, polyclonal rabbit anti-vimentin antibody (all from Abcam, Cambridge, MA, USA), and polyclonal rabbit anti-AQP-5 antibody (Biosynthesis Biotechnology, China). The co-cultured ADSCs were incubated overnight at 4°C with the following primary antibodies: polyclonal rabbit anti-amylase antibody (Abcam) and polyclonal rabbit anti-AQP-5 antibody (Biosynthesis Biotechnology). After washing with PBS, all of the cells were incubated with a fluorescein-conjugated goat anti-rabbit secondary antibody (Biosynthesis Biotechnology, China) at 37°C for 45 min. The samples were then washed and stained with 4',6'-diamidino-2-phenylindole hydrochloride (DAPI) (Biogot technology, Nanjing, China) to detect the nuclei. Finally, the stained cells were imaged under a fluorescence microscope (IX71, Olympus, Tokyo, Japan).

Western blotting

The confluent SGCs, ADSCs, and co-cultured ADSCs were washed with PBS and scraped into radioimmunoprecipitation assay (RIPA) buffer (Sigma-Aldrich). After two freeze-thaw cycles, the cells lysates were centrifuged at 12,000 rpm for 10 min. The protein concentration in the supernatants was quantified using a bicinchoninic acid (BCA) protein assay kit (Beyotime, Shanghai, China). Forty micrograms of total protein was loaded in each lane, and the proteins were separated by Tris-glycine sodium dodecyl sulfate (SDS)-polyacrylamide gel electrophoresis (Invitrogen Life Technologies, Carlsbad, CA, USA). The separated proteins were then transferred to polyvinylidene fluoride (PVDF) membranes (Millipore). The membranes were blocked with 5% (w/v) non-fat milk for 2 h before incubating overnight with the following antibodies at 4°C: Membranes containing proteins from confluent SGCs and ADSCs were probed with polyclonal rabbit anti-α-amylase antibody, polyclonal rabbit anti-CK 8 antibody, polyclonal rabbit anti-vimentin antibody (Abcam), and polyclonal rabbit anti-AQP-5 antibody (Biosynthesis Biotechnology). Membranes containing proteins from the co-cultured ADSCs were probed with polyclonal rabbit anti-α-amylase antibody (Abcam) and polyclonal rabbit anti-AQP-5 antibody (Biosynthesis Biotechnology). After four 5 min washes in TBS-Tween, the membranes were incubated at room temperature for 1 h with anti-rabbit horseradish peroxidase (HRP)-conjugated secondary antibodies (Cowin Biotech Co., Ltd., Beijing, China). The immunoreactive proteins were detected using the Western Light chemiluminescent detection system (Peiqing, Shanghai, China). Image J was used to evaluate the results of Western blots in ADSCs co-cultured in PRF condition medium for 7 days.

qRT-PCR

Quantification of mRNA was performed with qRT-PCR. *ALP, COLI, RUNX2*, and *OCN* mRNA

levels were analyzed in ADSCs that had been induced for osteogenesis. In SGCs and ADSCs, α-amylase, AQP-5, CK8, and vimentin mRNA levels were measured. Finally, in co-cultured ADSCs, α-amylase and AQP-5 mRNA levels were measured. Separately, total RNA was extracted from these cells using Trizol (Invitrogen Life Technologies), and RNA concentrations were measured spectrophotometrically. Reverse transcription was performed on 2-5 μg of total RNA using a RevertAid first strand cDNA synthesis kit (Takara, Bio, Otsu, Japan). Then, the cDNA was amplified with PCR using the SYBR® Premix Ex Taq™ II kit (Takara) in an ABI Prism 7500 sequence detection system (Applied Biosystems, Foster City, CA, USA). The qRT-PCR analysis was performed under the following conditions: denaturation at 95°C for 3 min, followed by 40 cycles at 95°C for 15 s and at 60°C for 30 s. Glyceraldehyde-3-phosphatedehydrogenase (GAPDH) was used as an internal control. All qRT-PCR was completed in triplicate. The following primers were used to investigate *ALP, COLI, RUNX2*, and *OCN* mRNA levels: ALP, forward 5'-TTGTGCCAGAGAAAGAGA-3' and reverse 5'-GTTTCAGGGCATTTTTCAAGGT-3'; COLI, forward 5'-GCTGGAGTTTCCGTGCCT-3' and reverse 5'-GACCTCGGGGACCCATTG-3'; RUNX2, forward 5'-AAATGCCTCCGCTGTTATGAA-3' and reverse 5'-AAGGTGAAACTCTTGCCTCGTC-3'; and OCN, forward 5'-TCTGCTCACTCTGCTGACCCTG-3' and reverse 5'-CGGAGTCTGTTCACTACCTTATTGC-3'. The primer sequences for α-amylase, CK8, AQP-5, and vimentin were as follows: α-amylase, forward 5'-GGTCACTGTGGAGCTCAGATCA-3' and reverse 5'-TTGCTATGCTGTTGGCAGTATTC-3'; CK8, forward 5'-GAACTAGAGTCCCGCCTGGAAG-3' and reverse 5'-GTTGTCCATAGACAGCACCACAGA-3'; AQP-5 forward 5'-GGTCACTGTGGAGCTCAGATCA-3' and reverse 5'-TTGCTATGCTGTTGGCAGTATTC-3'; and vimentin, forward 5'-AAAGCGTGGCTGCCAAGAA-3' and reverse 5'-ACCTGTCTCCGGTACTCGTTTGA-3'.

Statistical analysis

All data were collected from at least three independent experiments and are presented as the mean ± standard deviation (SD). Analysis of three or more groups was performed using one-way analysis of variance (ANOVA) with SPSS19.0 software. The control and experimental groups were compared with the Dunnett's test, and between group comparisons were analyzed with the least significant difference test. *P* values <0.05 were considered statistically significant. All graphs were created using GraphPad Prism 5 (Graph Pad Software Inc., La Jolla, CA, USA).

Results

Isolation and identification of ADSCs

ADSCs were isolated from C3H mouse inguinal fat pads using enzymatic digestion with collagenase. The isolated ADSCs were purified via subculture and exhibited spindle-shaped morphology (**Figure 1A**). Passage 3 ADSCs were used in all experiments. Next, the ADSCs were induced to differentiate into osteogenic, adipogenic, and chondrogenic lineages, and the cells were analyzed by flow cytometry to identify their mesenchymal stem cell properties. The flow cytometry analysis confirmed the expression of mesenchymal stem cell markers, including CD29 (99.56% ± 0.26%), CD44 (78.37 ± 1.41%), CD90 (94.57% ± 0.69%), and CD105 (95.97% ± 1.30%). No significant expression of CD31 (2.00% ± 0.50%), CD34 (2.50% ± 0.57%), or CD45 (2.77% ± 0.65%) was observed (**Figure 1B**). Osteogenic differentiation was assessed on the basis of calcium deposits, which were identified with Alizarin red staining (**Figure 1C**). Adipogenic differentiation was confirmed on the basis of lipid droplet production, which was detected with Oil Red-O staining (**Figure 1D**). Finally, positive staining with Alcian blue indicated chondrogenic differentiation (**Figure 1E**). Collectively, these results suggested that multipotent ADSCs had been cultured.

Characteristics of C3H mouse SGCs

The SGCs obtained from 4-week-old C3H mice had round or polygonal morphologies and adopted a cobblestone arrangement when grown to confluence after 10 days of culture. The SGCs exhibited characteristic epithelial cell-like structures (**Figure 2A**). The sub-cultured, passage 1 SGCs maintained the same morphological characteristics as the primary passage SGCs (**Figure 2B**). Immunofluorescence staining revealed that α-amylase, AQP-5, and CK8 proteins were expressed in the SGCs (**Figure 2C**), and expression of the corresponding genes was confirmed using qRT-PCR (**Figure 2D**). Western blotting also confirmed protein ex-

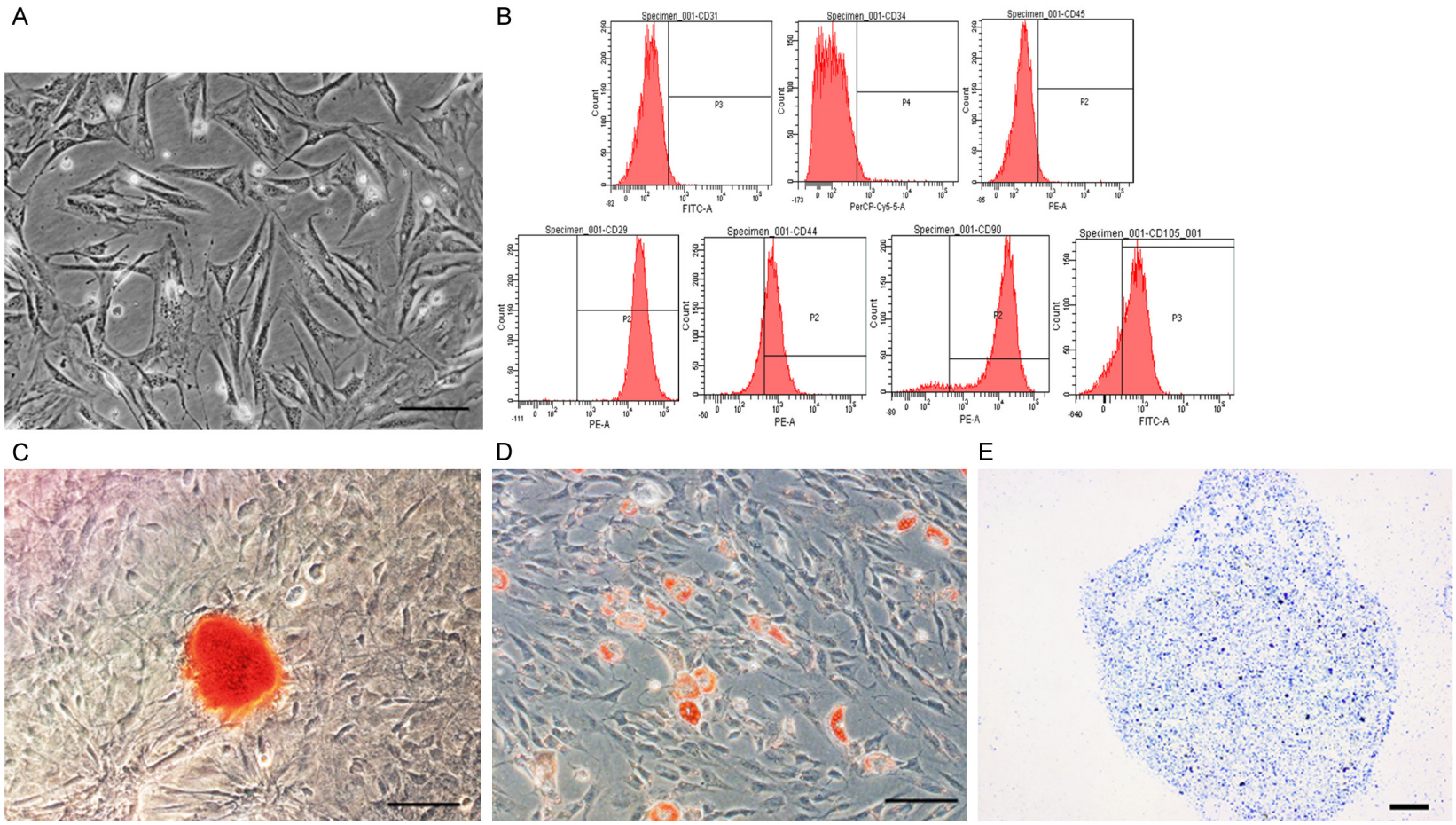

Figure 1. Identification of ADSCs. A. Representative phase image of passage 3 ADSCs that exhibited spindle-like morphology. B. Flow cytometry analysis of ADSCs that were positive for CD29, CD44, CD90, and CD105 and negative for CD31, CD34, and CD45. C. Alizarin red staining confirmed osteogenic induction of ADSCs. D. Adipogenesis of ADSCs was confirmed by Oil Red-O staining that indicated the production of lipid droplets. E. Alcian blue staining confirmed chondrogenic induction of ADSCs. Scale bar = 100 μm.

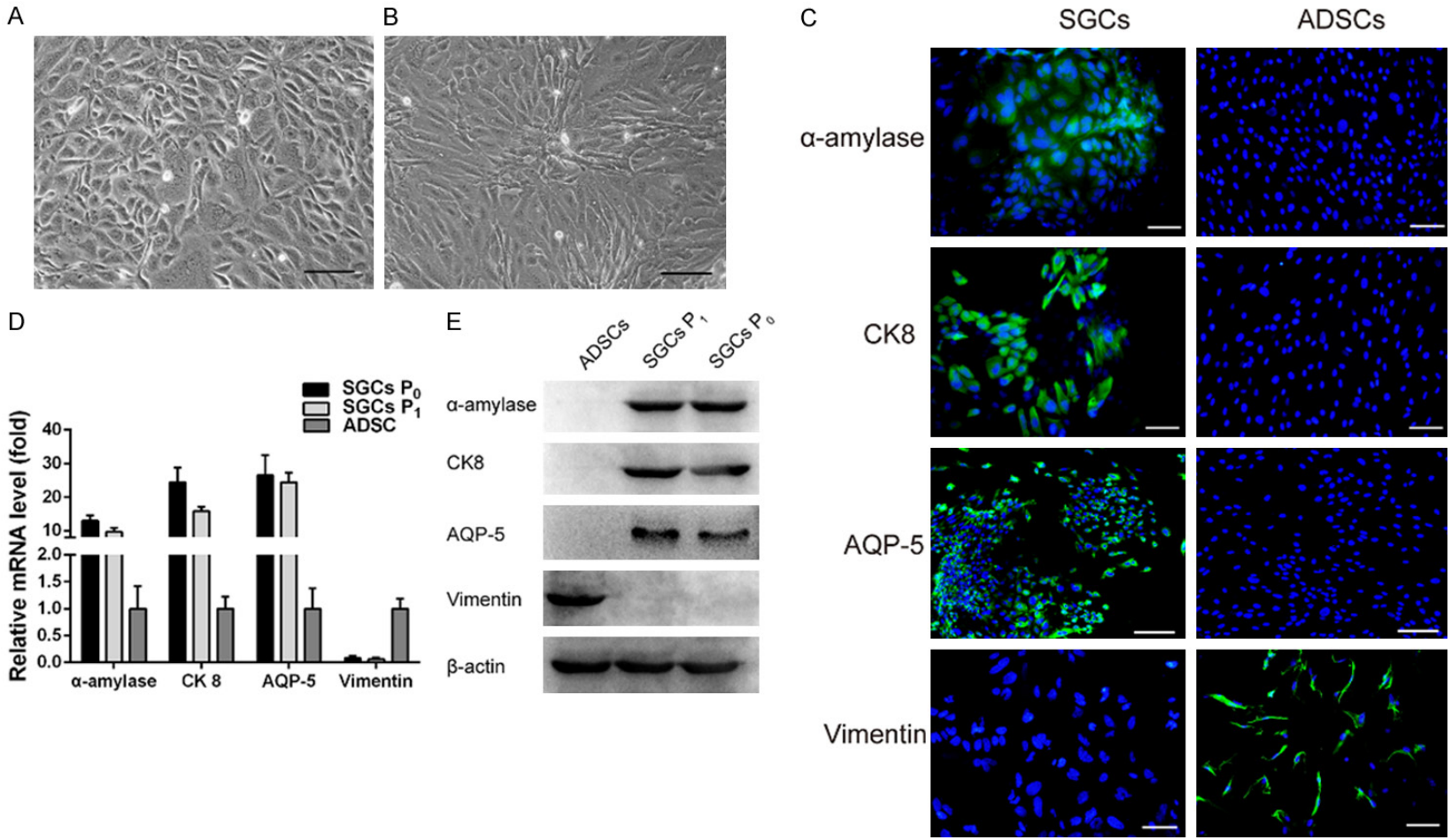

Figure 2. Characterization of SGCs. ADSCs were the control cells. A and B. Morphology of primary SGCs (SGCs P_0) and passage 1 SGCs (SGCs P_1), respectively. C. IF staining of α-amylase, CK8, and AQP-5 was positive for SGCs and negative for ADSCs. IF staining of vimentin was negative for SGCs, but positive for ADSCs. D. Expression levels of α-amylase, CK8, and AQP-5 mRNA in SGCs. E. Western blotting confirmed the expression of α-amylase, CK8, and AQP-5 in SGCs. Scale bar = 100 μm.

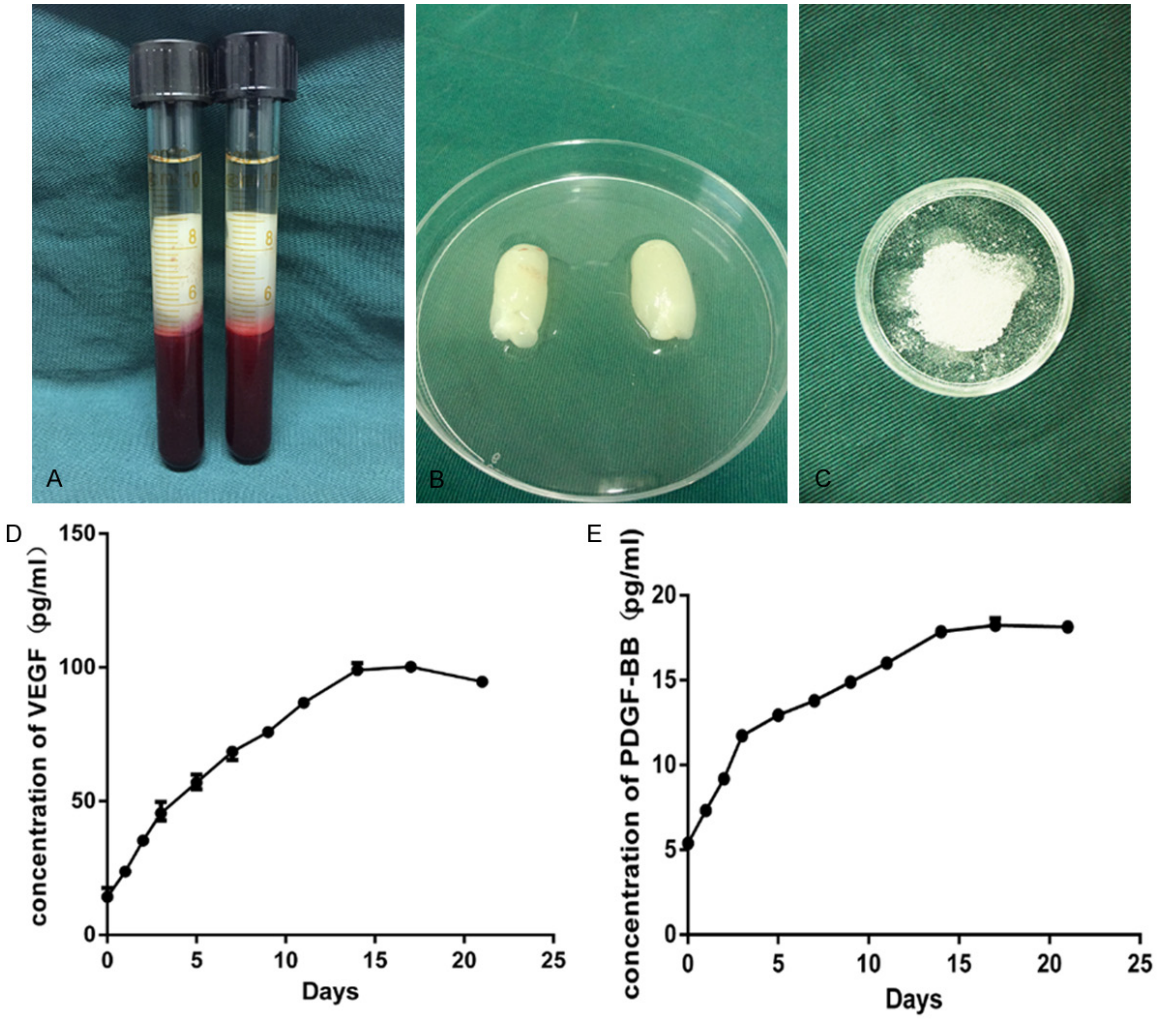

Figure 3. PRF appearance and the release of VEGF and PDGF-BB from PRF. (A) The middle layer after centrifugation contained the PRF clot. (B) Fresh PRF isolated from blood samples. (C) Lyophilized PRF particles. ELISA results for (D) VEGF and (E) PDGF-BB released from lyophilized PRF.

pression of α-amylase, AQP-5, and CK8 (**Figure 2E**). Notably, SGCs did not express vimentin, and control ADSCs expressed vimentin, but did not express α-amylase, AQP-5, or CK8.

VEGF and PDGF-BB levels in lyophilized PRF

After centrifugation at 3,000 rpm for 10 min, the blood samples were separated into three distinct layers. The middle layer contained gel-like clots of PRF (**Figure 3A** and **3B**). The clots were then freeze-dried for 24 h and the lyophilized PRF was ground into small particles (**Figure 3C**). The release of VEGF and PDGF-BB was quantified using an ELISA, and the data is presented in **Figure 3D** and **3E**. The results indicate that both growth factors were continuously released for 15 days. After day 15, no obvious release of either growth factor is observed. The slopes of both release curves for the first 3 days were greater than the slopes from day 5 to 15, indicating an initial rapid release of both growth factors. At all time points, the concentration of released VEGF was higher than PDGF-BB.

Proliferation and osteogenic differentiation of ADSCs that were stimulated by lyophilized PRF

Cell growth curves were plotted (**Figure 4A**), and the stimulatory effect of lyophilized PRF on ADSC proliferation was evident. The MTT assay absorbance values, which are indicative of cell metabolic activity, on day 1, 2, and 8 were compared statistically (**Figure 4B**). On day 1, there was no significant difference between any two

groups, which indicated that the initial cell numbers were identical. Compared to the control group, the ADSC groups with 0.5%, 1%, and 3% PRF-conditioned medium had significantly higher absorbance values on day 2 and day 8, indicating increased proliferation (P<0.05). However, the ADSC groups with 20%, 50%, and 80% PRF-conditioned medium had significantly lower absorbance values when compared to the control group, suggesting that these cells exhibited attenuated proliferation (P<0.05). The absorbance values of the ADSC groups that were cultured in 5%, 7%, and 10% PRF-conditioned medium were not significantly different from the control group (P>0.05).

The expression of osteogenesis-related genes in ADSCs cultured with conditioned medium was evaluated using qRT-PCR and compared to the expression in control cells (**Figure 4C**). Osteogenic induction was significantly enhanced in groups with 0.5%, 1%, 3%, and 5% PRF-conditioned medium. In these groups, the mRNA levels of four osteogenesis-related genes, *ALP, COLI, RUNX2*, and *OCN*, were greater than the control group (P<0.05). Among the four groups, the group cultured in 1% PRF-conditioned medium exhibited the greatest enhancement of osteogenic gene expression. The group with 7% PRF-conditioned medium had increased *ALP, RUNX2*, and *OCN* mRNA levels and decreased *COLI* mRNA. *ALP* and *RUNX2* expression was suppressed in the 10% PRF-conditioned medium group. After 21 days of osteogenic induction, mineralization was assessed with Alizarin red staining (**Figure 4D**). We observed mineralized nodules in all groups. However, the ADSCs culture with 0.5%, 1%, 3%, 5%, and 7% PRF-conditioned medium had more nodules when visually compared to the control group.

Transdifferentiation of ADSCs into SGALCs

ADSC morphology and α-amylase and AQP-5 expression were evaluated on co-culture day 7, 14, and 21. In the control groups, ADSCs exhibited a uniform fibroblast-like morphology and a high-density cell arrangement. Interestingly, a portion of the ADSCs that were co-cultured with SGCs appeared to lose their fibroblast-like morphology. Instead, these cells became more polygonal, and the number of cells that exhibited this morphology increased with the co-culture duration (**Figure 5A**). Immunofluorescence staining confirmed the expression of α-amylase and AQP-5 by the co-cultured ADSCs, but these proteins were not expressed by the control cells (**Figure 5B** and **5C**). DAPI staining was used to identify nuclei and the nuclei of α-amylase-positive ADSCs in five different areas were counted to calculate ADSC and SGALC transdifferentiation rates. The transdifferentiation rates of ADSCs co-cultured for 7, 14, and 21 days were 22.87 ± 1.66%, 40.56 ± 1.74%, and 49.84 ± 1.93%, respectively. Increased α-amylase and AQP-5 expression were also confirmed by western blotting and qRT-PCR (**Figure 5D** and **5E**).

The effect of PRF on ADSC transdifferentiation within the co-culture system was also evaluated. In a 7-day co-culture system, ADSCs were co-cultured with SGCs in PRF-conditioned medium. Expression of α-amylase and AQP-5 were visualized with immunofluorescence staining (**Figure 6A**) and the transdifferentiation rates were calculated. The ADSC groups treated with 0.5%, 1%, 3%, and 5% PRF-conditioned medium had transdifferentiation rates of 30.39 ± 1.51%, 36.20 ± 1.33%, 31.43 ± 1.26%, and 28.78 ± 0.83%, respectively. Notably, the addition of PRF significantly increased the transdifferentiation rate when compared to ADSCs co-cultured without PRF-conditioned medium (22.87 ± 1.66%, P<0.05). The group treated with 1% PRF-conditioned medium had the highest transdifferentiation rate. Western blotting and qRT-PCR confirmed the expression of α-amylase and AQP-5 in ADSCs co-cultured in PRF-conditioned medium (**Figure 6B-D**). Significantly higher expression of α-amylase and AQP-5 was measured in the PRF-cultured groups when compared to the co-culture groups without PRF-conditioned medium (P<0.05). The expression of α-amylase and AQP-5 was not observed in ADSCs co-cultured without SGCs both in the presence and absence of PRF-conditioned medium.

Discussion

Radiotherapy for head and neck cancer causes irreversible SGs hypofunction, a condition without any effective cure. Importantly, stem cells, including ADSCs, are reported to have immense potential for restoring the morphology and function of radiation-damaged SGs [36], and the process is augmented by PRF. However, the precise mechanisms of ADSC-induced recovery

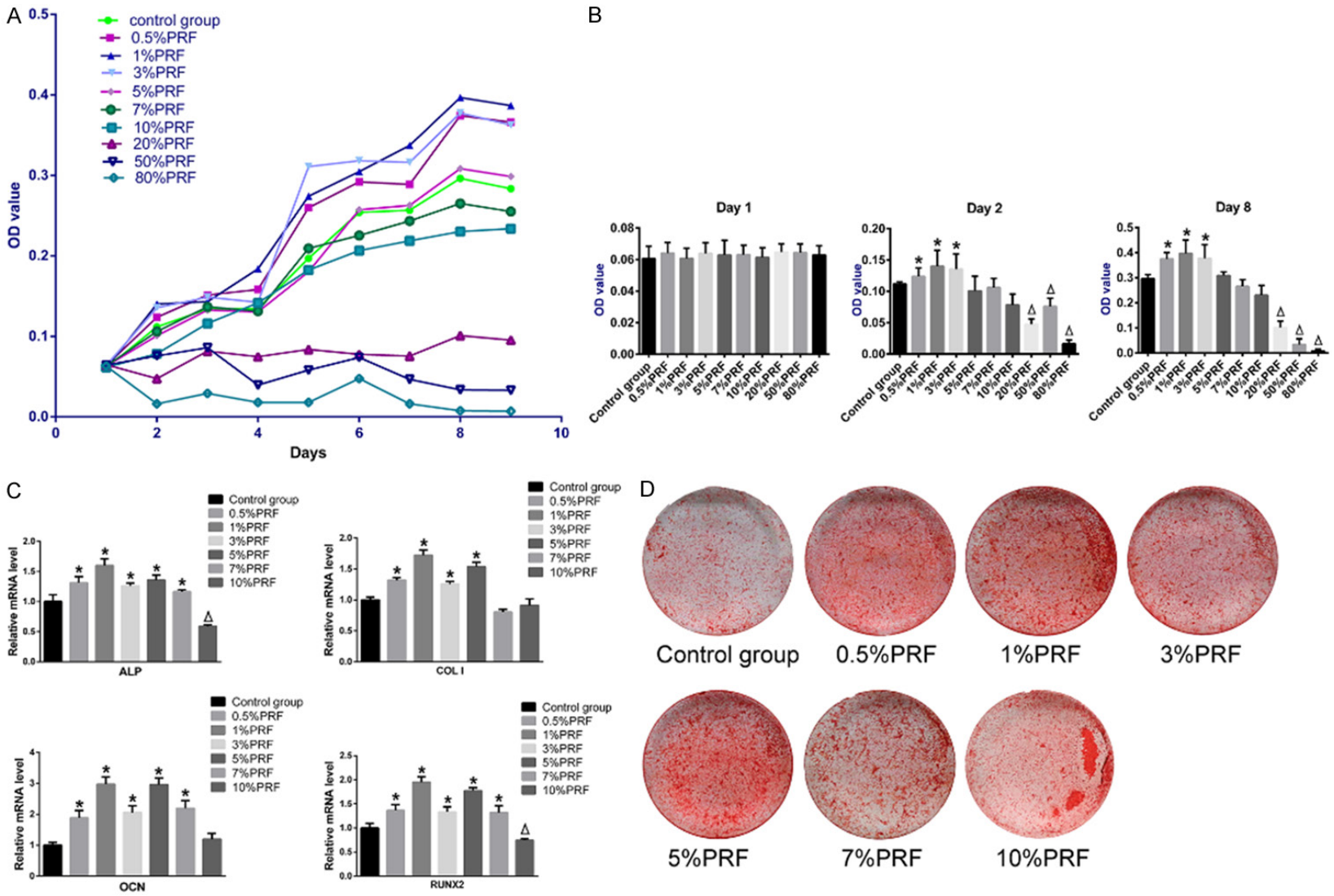

Figure 4. Effects of PRF on ADSC proliferation and osteogenesis. Groups without PRF-conditioned medium were controls. A. Cell proliferation of different ADSC groups cultured in PRF-conditioned medium were measured with the MTT assay. B. Statistical analysis of MTT assay OD values on day 1, 2, and 8 of ADSCs grown in PRF-conditioned medium. C. The relative mRNA levels of *ALP, COLI, RUNX2* and *OCN* in ADSCs from different PRF-conditioned medium groups. D. Alizarin red staining of ADSCs from different PRF-conditioned medium groups after 21-days of osteogenic induction. *P<0.05 indicates a significant increase; ΔP<0.05 indicates a significant decrease, when compared to control groups by one-way analysis of variance.

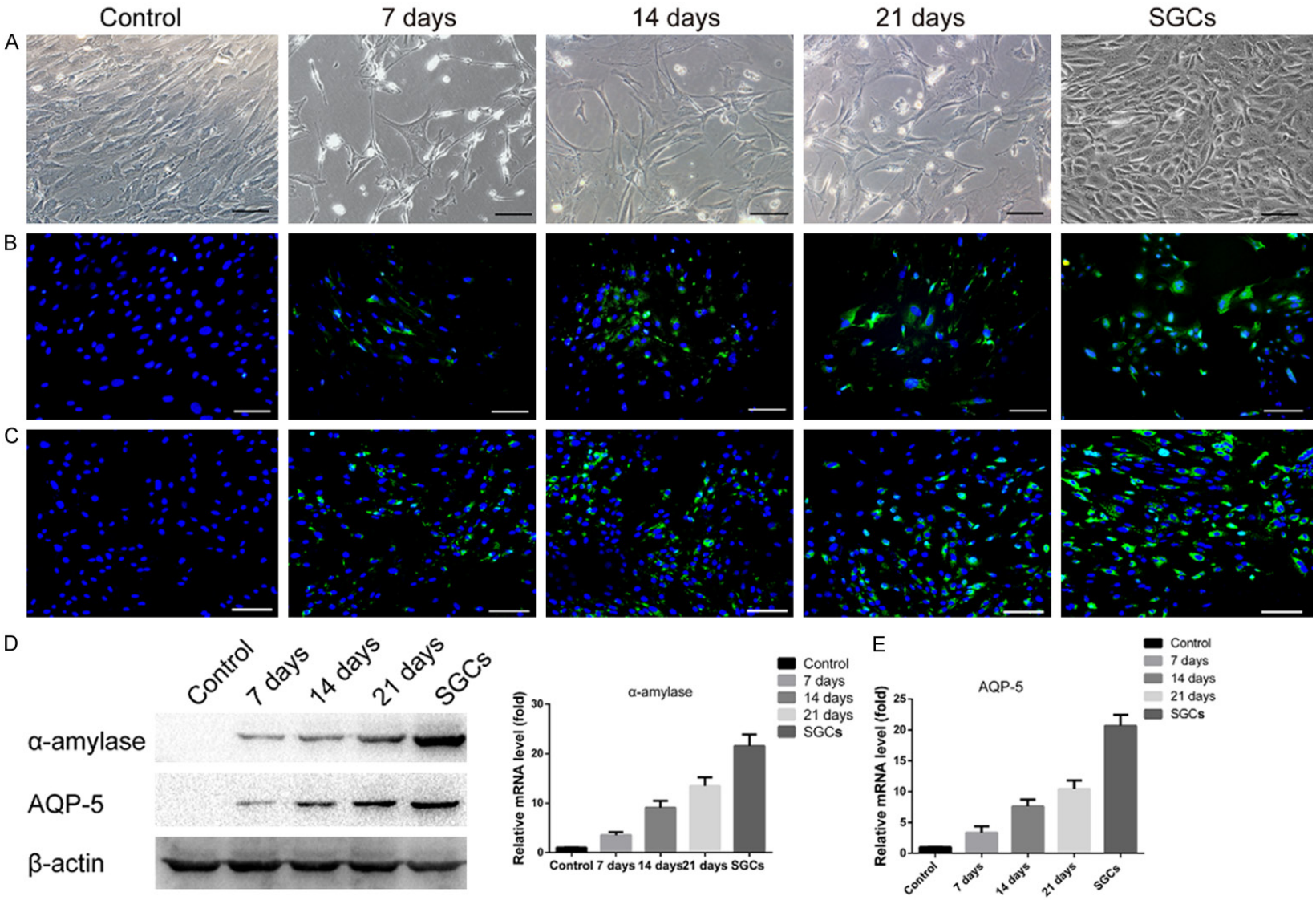

Figure 5. Transdifferentiation of co-cultured ADSCs into SGALCs. ADSCs co-cultured without SGCs were negative controls and SGCs were positive controls. (A) Morphological changes in ADSCs were observed after co-culture. IF staining confirmed the expression of (B) α-amylase and (C) AQP-5 in co-cultured ADSCs. Green indicates the protein of interest and blue indicates nuclear staining with DAPI. (D) The expression of α-amylase and AQP-5 after different amounts of time in the co-culture system was evaluated by western blotting. (E) The relative mRNA levels of α-amylase and AQP-5 increased with amount of time in the co-culture system. Scale bar = 100 μm.

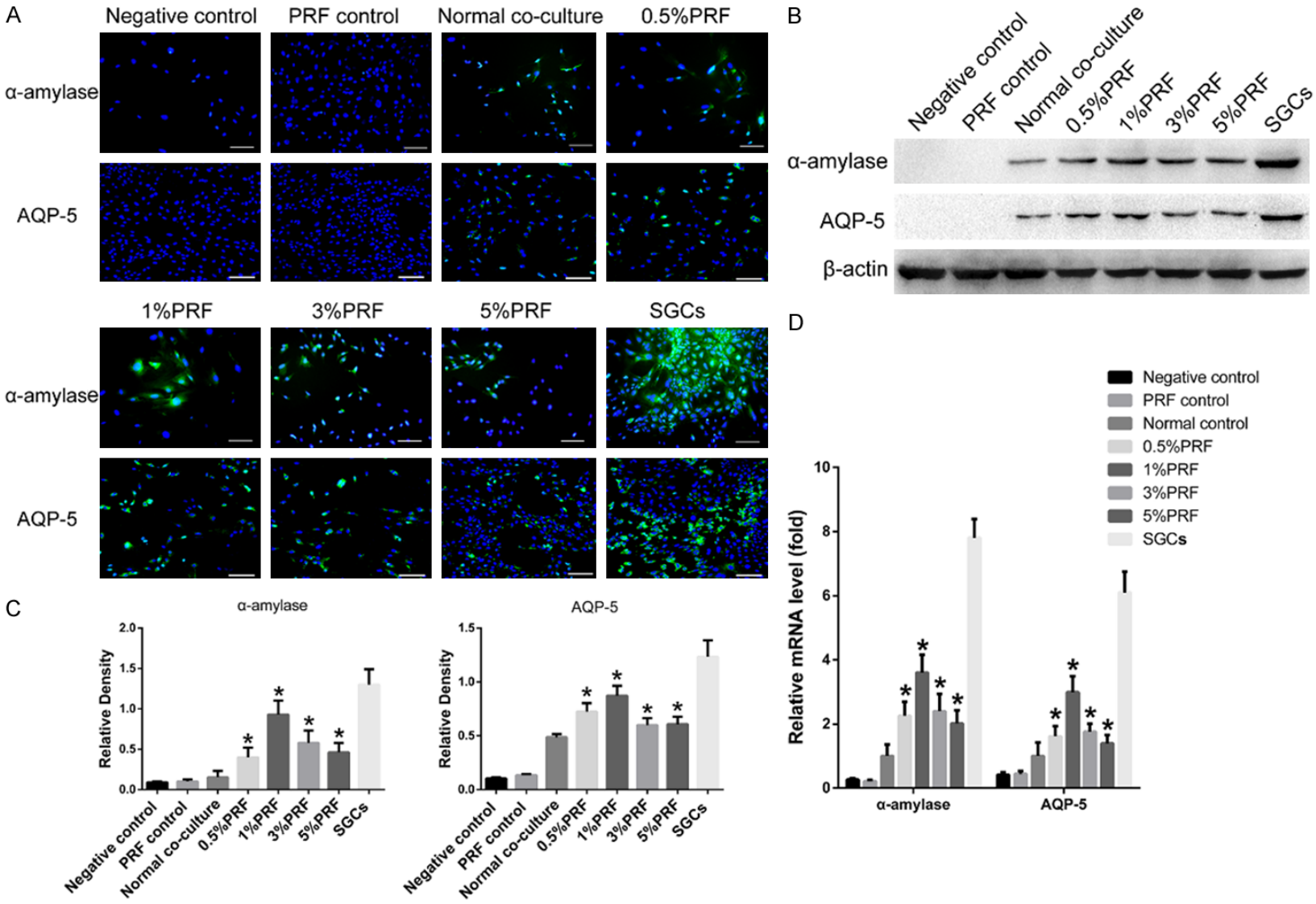

Figure 6. Effect of PRF on the transdifferentiation of ADSCs into SGALCs. A. IF staining of α-amylase and AQP-5 expression in different PRF-conditioned medium and control groups. B. The expression of α-amylase and AQP-5 in ADSCs from different PRF-conditioned medium and control groups was evaluated by western blotting. C. ImageJ analysis of the western blotting results revealed higher expression of α-amylase and AQP-5 in ADSCs from PRF-conditioned medium groups. D. Relative mRNA levels of α-amylase and AQP-5 were higher in ADSCs from PRF-conditioned medium groups. Scale bar = 100 μm. *P<0.05 indicates a significant increase when compared with the normal co-culture group by one-way analysis of variance.

of SG function are still uncertain. Several studies suggest that transdifferentiation, paracrine effects, angiogenesis, and cell fusion may contribute to the protective and remedial roles of ADSCs in SG irradiation injuries [37]. We hypothesize that cellular transdifferentiation is the most direct way for ADSCs to preserve and restore SGs function. In the present study, we demonstrated that ADSCs can transdifferentiate into SGALCs, and that PRF enhanced the in vitro transdifferentiation.

Similar to BMMSCs, ADSCs are also multipotent stem cells. In this study, a cell population isolated from the mouse inguinal fat pad exhibited a fibroblast-like morphology, possessed adipogenic and osteogenic potential, and expressed high levels of the stem cell-related antigens (CD29, CD44, CD90, and CD105). These results are consistent with previous studies [33, 38] and suggest that the isolated cell population was ADSCs. Prior studies indicate that ADSCs can transdifferentiate into many different cell types during co-culture including Schwann-like cells and cardiomyocyte-like cells [30, 31]. In this study, ADSCs transdifferentiated into SGALCs during indirect co-culture with SGCs. The expression of α-amylase and AQP-5, which are essential for SG acinar cell function, were used to confirm ADSC transdifferentiation. Notably, α-amylase and AQP-5 expression was not detected in ADSCs that were cultured in the absence SGCs.

Similar to the experimental set-up employed by other studies, a double-chamber system for indirect co-culture using Transwell inserts with a pore size of 0.4 μm allowed SGCs to create the correct microenvironment for ADSC induction. SGCs in the upper chamber were mixed cell populations that expressed α-amylase, AQP-5, and CK8. ADSCs were seeded in the lower chamber. We hypothesized that the initial ratio of the two cell types could be an important factor that affects ADSC transdifferentiation. A prior study reported that BMMSCs transdifferentiated into SG acinar cells when they were co-cultured with acinar cells at an acinar cell and BMMSC ratio of four to one [39]. In addition, in a preliminary study, we observed that ADSC transdifferentiation was impeded when the SGC number was low. Excess SGCs suppressed proliferation and caused ADSC death. Therefore, an SGC and ADSC ratio of four to one for SGCs and ADSCs was used in the current study.

The SGCs in the upper Transwell inserts were essential for ADSC transdifferentiation. The transdifferentiation process can be initiated by stochastic fluctuations, gene regulation, and induction [40]. In addition to direct transfection with specific genes that induce transdifferentiation, the transdifferentiation of ADSCs can also be induced by a co-culture system. Co-cultured ADSCs may undergo stochastic fluctuations in gene regulation under the influence of the SGC-supplied microenvironment. The soluble factors released by SGCs induce the downregulation of ADSC-specific genes and activate SGC-specific genes in ADSCs. However, the factors and related pathways remain unknown.

After 7, 14, and 21 days of co-culture, partial ADSCs lost their fibroblast-like morphology and became more polygonal in shape. However, not all ADSCs transdifferentiated into SGALCs, which was revealed by α-amylase and AQP-5 expression in partial ADSCs. These results were also confirmed by immunofluorescence staining, western blotting, and qRT-PCR. Our results demonstrated that the transdifferentiation rates of ADSCs increased with co-culture time and that about 50% of the co-cultured ADSCs expressed α-amylase after 21 days, which was similar to results observed in BMMSCs [39]. The increase in ADSCs transdifferentiation rate from 7 to 14 days of co-culture was higher than the rate from 14 to 21 days of co-culture, which indicated that a rapid transdifferentiation process occurred during the earlier stage of co-culture.

PRF can promote the proliferation and differentiation of many different cell types in vitro [26, 27, 41]. Our results suggest that lyophilized PRF exhibits characteristics that are similar to fresh PRF and still releases growth factors, including VEGF and PDGF-BB. Importantly, lyophilized PRF is easier to store and would therefore, be easier to administer in a clinical setting. The conditioned medium extracted from lyophilized PRF promoted ADSCs proliferation and differentiation in a dose-dependent manner. The medium with 1% PRF had the greatest enhancing effect and medium with >10% PRF had suppressive effects. Furthermore, we also observed a significant increase in ADSCs transdifferentiation rates on day 7 in the co-culture sys-

tem when PRF-conditioned medium was used. Increased protein levels of α-amylase and AQP-5, and their related genes, were detected using western blotting and qRT-PCR, respectively. These data indicate that PRF-mediates ADSCs transdifferentiation. In addition to its in vitro transdifferentiation effects, several studies report that PRF can also be used in tissue repair and regeneration. The effects of PRF are attributed to the abundance of vital growth factors trapped in its complex three-dimensional structure. The three most important growth factors in PRF are PDGF, TGF, and IGF. These growth factors have important roles related to cell proliferation and differentiation and may contribute to increased transdifferentiation of ADSCs into SGALCs.

Although we report the transdifferentiation of ADSCs into SGALCs in vitro, recapitulating the results in vivo remains uncertain. Therefore, additional studies are warranted to investigate the feasibility of in vivo ADSCs transdifferentiation. In addition, due to limitations caused by the maximum in vitro culture time for both cell types used here, the co-culture study only lasted for 21 days. Longer studies could provide additional interesting results. Finally, the molecular mechanisms of PRF-mediated ADSC transdifferentiation into SGALCs should be the focus of a future study.

In conclusion, our data confirmed that ADSCs transdifferentiate into SGALCs and that the process is promoted by PRF. These observations may partially explain why ADSCs ameliorate radiation-induced damage to SGs. Furthermore, the results establish a beneficial role for PRF when combined with ADSCs to improve the function of SGs damaged by radiation. Finally, the data suggests that ADSCs may have translational applications for the treatment of salivary gland hypofunction.

Acknowledgements

This study was supported by the National Natural Science Foundation of China (Grant number: 31170942).

Disclosure of conflict of interest

None.

Address correspondence to: Dr. Bin Liu, State Key Laboratory of Military Stomatology, Laboratory Animal Center, School of Stomatology, The Fourth Military Medical University, 145 West Changle Road, Xi'an 710032, PR China. Tel: +86-029-84776175; Fax: +86-029-84776175; E-mail: kqyljd_liu@126.com; Dr. Yan-Pu Liu, State Key Laboratory of Military Stomatology & National Clinical Research Center for Oral Diseases & Shaanxi Clinical Research Center for Oral Diseases, Department of Oral and Maxillofacial Surgery, School of Stomatology, The Fourth Military Medical University, 145 West Changle Road, Xi'an 710032, PR China. Tel: +86-029-84772532; Fax: +86-029-83224470; E-mail: liuyanpu@fmmu.edu.cn

References

[1] Humphrey SP and Williamson RT. A review of saliva: normal composition, flow, and function. J Prosthet Dent 2001; 85: 162-169.

[2] Jensen SB, Pedersen AM, Vissink A, Andersen E, Brown CG, Davies AN, Dutilh J, Fulton JS, Jankovic L, Lopes NN, Mello AL, Muniz LV, Murdoch-Kinch CA, Nair RG, Napeñas JJ, Nogueira-Rodrigues A, Saunders D, Stirling B, von Bültzingslöwen I, Weikel DS, Elting LS, Spijkervet FK, Brennan MT; Salivary Gland Hypofunction/Xerostomia Section, Oral Care Study Group, Multinational Association of Supportive Care in Cancer (MASCC)/International Society of Oral Oncology (ISOO). A systematic review of salivary gland hypofunction and xerostomia induced by cancer therapies: prevalence, severity and impact on quality of life. Support Care Cancer 2010; 18: 1039-1060.

[3] Chitapanarux I, Kamnerdsupaphon P, Tharavichitkul E, Sumitsawan Y, Sittitrai P, Pattarasakulchai T, Lorvidhaya V, Sukthomya V, Pukanhaphan N and Traisatit P. Effect of oral pilocarpine on post-irradiation xerostomia in head and neck cancer patients: a single-center, single-blind clinical trial. J Med Assoc Thai 2008; 91: 1410-1415.

[4] Momm F, Volegova-Neher NJ, Schulte-Monting J and Guttenberger R. Different saliva substitutes for treatment of xerostomia following radiotherapy. A prospective crossover study. Strahlenther Onkol 2005; 181: 231-236.

[5] Gerlach NL, Barkhuysen R, Kaanders JH, Janssens GO, Sterk W and Merkx MA. The effect of hyperbaric oxygen therapy on quality of life in oral and oropharyngeal cancer patients treated with radiotherapy. Int J Oral Maxillofac Surg 2008; 37: 255-259.

[6] Johnstone PA, Peng YP, May BC, Inouye WS and Niemtzow RC. Acupuncture for pilocarpine-resistant xerostomia following radiotherapy for head and neck malignancies. Int J Radiat Oncol Biol Phys 2001; 50: 353-357.

[7] Vissink A, Mitchell JB, Baum BJ, Limesand KH, Jensen SB, Fox PC, Elting LS, Langendijk JA, Coppes RP and Reyland ME. Clinical management of salivary gland hypofunction and xerostomia in head-and-neck cancer patients: successes and barriers. Int J Radiat Oncol Biol Phys 2010; 78: 983-991.

[8] Zhu Y, Liu T, Song K, Fan X, Ma X and Cui Z. Adipose-derived stem cell: a better stem cell than BMSC. Cell Biochem Funct 2008; 26: 664-675.

[9] Purandare B, Teklemariam T, Zhao L and Hantash BM. Temporal HLA profiling and immunomodulatory effects of human adult bone marrow- and adipose-derived mesenchymal stem cells. Regen Med 2014; 9: 67-79.

[10] Huang SP, Huang CH, Shyu JF, Lee HS, Chen SG, Chan JY and Huang SM. Promotion of wound healing using adipose-derived stem cells in radiation ulcer of a rat model. J Biomed Sci 2013; 20: 51.

[11] Pieri F, Lucarelli E, Corinaldesi G, Aldini NN, Fini M, Parrilli A, Dozza B, Donati D and Marchetti C. Dose-dependent effect of adipose-derived adult stem cells on vertical bone regeneration in rabbit calvarium. Biomaterials 2010; 31: 3527-3535.

[12] Yin F, Cai J, Zen W, Wei Y, Zhou W, Yuan F, Singh SR and Wei Y. Cartilage regeneration of adipose-derived stem cells in the TGF-beta1-immobilized PLGA-gelatin scaffold. Stem Cell Rev 2015; 11: 453-459.

[13] Watanabe Y, Sasaki R, Matsumine H, Yamato M and Okano T. Undifferentiated and differentiated adipose-derived stem cells improve nerve regeneration in a rat model of facial nerve defect. J Tissue Eng Regen Med 2017; 11: 362-374.

[14] Koellensperger E, Niesen W, Kolbenschlag J, Gramley F, Germann G and Leimer U. Human adipose tissue derived stem cells promote liver regeneration in a rat model of toxic injury. Stem Cells Int 2013; 2013: 534263.

[15] Diaz-Herraez P, Saludas L, Pascual-Gil S, Simon-Yarza T, Abizanda G, Prosper F, Garbayo E and Blanco-Prieto MJ. Transplantation of adipose-derived stem cells combined with neuregulin-microparticles promotes efficient cardiac repair in a rat myocardial infarction model. J Control Release 2017; 249: 23-31.

[16] Kojima T, Kanemaru S, Hirano S, Tateya I, Ohno S, Nakamura T and Ito J. Regeneration of radiation damaged salivary glands with adipose-derived stromal cells. Laryngoscope 2011; 121: 1864-1869.

[17] Xiong X, Shi X and Chen F. Human adipose tissuederived stem cells alleviate radiationinduced xerostomia. Int J Mol Med 2014; 34: 749-755.

[18] Lim JY, Ra JC, Shin IS, Jang YH, An HY, Choi JS, Kim WC and Kim YM. Systemic transplantation of human adipose tissue-derived mesenchymal stem cells for the regeneration of irradiation-induced salivary gland damage. PLoS One 2013; 8: e71167.

[19] Dohan DM, Choukroun J, Diss A, Dohan SL, Dohan AJ, Mouhyi J and Gogly B. Platelet-rich fibrin (PRF): a second-generation platelet concentrate. Part I: technological concepts and evolution. Oral Surg Oral Med Oral Pathol Oral Radiol Endod 2006; 101: e37-44.

[20] Dohan DM, Choukroun J, Diss A, Dohan SL, Dohan AJ, Mouhyi J and Gogly B. Platelet-rich fibrin (PRF): a second-generation platelet concentrate. Part II: platelet-related biologic features. Oral Surg Oral Med Oral Pathol Oral Radiol Endod 2006; 101: e45-50.

[21] Ding Y, Cui L, Zhao Q, Zhang W, Sun H and Zheng L. Platelet-rich fibrin accelerates skin wound healing in diabetic mice. Ann Plast Surg 2017; 79: e15-e19.

[22] Dohle E, El Bagdadi K, Sader R, Choukroun J, James Kirkpatrick C and Ghanaati S. PRF-based matrices to improve angiogenesis in an in vitro co-culture model for bone tissue engineering. J Tissue Eng Regen Med 2017; 12: 598-610.

[23] Li Q, Reed DA, Min L, Gopinathan G, Li S, Dangaria SJ, Li L, Geng Y, Galang MT, Gajendrareddy P, Zhou Y, Luan X and Diekwisch TG. Lyophilized platelet-rich fibrin (PRF) promotes craniofacial bone regeneration through Runx2. Int J Mol Sci 2014; 15: 8509-8525.

[24] Chien CS, Ho HO, Liang YC, Ko PH, Sheu MT and Chen CH. Incorporation of exudates of human platelet-rich fibrin gel in biodegradable fibrin scaffolds for tissue engineering of cartilage. J Biomed Mater Res B Appl Biomater 2012; 100: 948-955.

[25] Li Q, Pan S, Dangaria SJ, Gopinathan G, Kolokythas A, Chu S, Geng Y, Zhou Y and Luan X. Platelet-rich fibrin promotes periodontal regeneration and enhances alveolar bone augmentation. Biomed Res Int 2013; 2013: 638043.

[26] He L, Lin Y, Hu X, Zhang Y and Wu H. A comparative study of platelet-rich fibrin (PRF) and platelet-rich plasma (PRP) on the effect of proliferation and differentiation of rat osteoblasts in vitro. Oral Surg Oral Med Oral Pathol Oral Radiol Endod 2009; 108: 707-713.

[27] Dohan Ehrenfest DM, Doglioli P, de Peppo GM, Del Corso M and Charrier JB. Choukroun's platelet-rich fibrin (PRF) stimulates in vitro proliferation and differentiation of human oral bone mesenchymal stem cell in a dose-dependent way. Arch Oral Biol 2010; 55: 185-194.

[28] Huang FM, Yang SF, Zhao JH and Chang YC. Platelet-rich fibrin increases proliferation and

differentiation of human dental pulp cells. J Endod 2010; 36: 1628-1632.
[29] Li Z, Wang Y, Xing H, Wang Z, Hu H, An R, Xu H, Liu Y and Liu B. Protective efficacy of intravenous transplantation of adipose-derived stem cells for the prevention of radiation-induced salivary gland damage. Arch Oral Biol 2015; 60: 1488-1496.
[30] Zhu Y, Liu T, Song K, Ning R, Ma X and Cui Z. ADSCs differentiated into cardiomyocytes in cardiac microenvironment. Mol Cell Biochem 2008; 324: 117-129.
[31] Wei Y, Gong K, Zheng Z, Liu L, Wang A, Zhang L, Ao Q, Gong Y and Zhang X. Schwann-like cell differentiation of rat adipose-derived stem cells by indirect co-culture with Schwann cells in vitro. Cell Prolif 2010; 43: 606-616.
[32] Liu J, Huang J, Lin T, Zhang C and Yin X. Cell-to-cell contact induces human adipose tissue-derived stromal cells to differentiate into urothelium-like cells in vitro. Biochem Biophys Res Commun 2009; 390: 931-936.
[33] Taha MF and Hedayati V. Isolation, identification and multipotential differentiation of mouse adipose tissue-derived stem cells. Tissue Cell 2010; 42: 211-216.
[34] Park YJ, Koh J, Gauna AE, Chen S and Cha S. Identification of regulatory factors for mesenchymal stem cell-derived salivary epithelial cells in a co-culture system. PLoS One 2014; 9: e112158.
[35] Choukroun JAF, Schoeffler C, Vervelle A. Une opportunite' en paro-implantologie: le PRF. Implantodontie 2001; 42: 55-62.
[36] Yoo C, Vines JB, Alexander G, Murdock K, Hwang P and Jun HW. Adult stem cells and tissue engineering strategies for salivary gland regeneration: a review. Biomater Res 2014; 18: 9.
[37] Jensen DH, Oliveri RS, Trojahn Kolle SF, Fischer-Nielsen A, Specht L, Bardow A and Buchwald C. Mesenchymal stem cell therapy for salivary gland dysfunction and xerostomia: a systematic review of preclinical studies. Oral Surg Oral Med Oral Pathol Oral Radiol 2014; 117: 335-342.
[38] Gimble J and Guilak F. Adipose-derived adult stem cells: isolation, characterization, and differentiation potential. Cytotherapy 2003; 5: 362-369.
[39] Lin CY, Lee BS, Liao CC, Cheng WJ, Chang FM and Chen MH. Transdifferentiation of bone marrow stem cells into acinar cells using a double chamber system. J Formos Med Assoc 2007; 106: 1-7.
[40] Xu L, Zhang K and Wang J. Exploring the mechanisms of differentiation, dedifferentiation, reprogramming and transdifferentiation. PLoS One 2014; 9: e105216.
[41] Dohan Ehrenfest DM, Diss A, Odin G, Doglioli P, Hippolyte MP and Charrier JB. In vitro effects of Choukroun's PRF (platelet-rich fibrin) on human gingival fibroblasts, dermal prekeratinocytes, preadipocytes, and maxillofacial osteoblasts in primary cultures. Oral Surg Oral Med Oral Pathol Oral Radiol Endod 2009; 108: 341-352.